Multi-period AC-QP Optimal Power Flow Including Storage

Jennifer F. Marley Ian A. Hiskens
Department of Electrical Engineering and Computer Science
University of Michigan
Ann Arbor, MI 48104
Email: {jkfelder,hiskens}@umich.edu

***Abstract*—There is an increasing need for integrating renewable generation sources into electricity networks. To take advantage of the economic and environmental benefits offered by renewable sources, storage devices are important to mitigate their inherent variability. However, the physical properties of storage devices require operation to be optimized over a finite horizon. This paper provides a multi-period optimal power flow (OPF) formulation including both wind generation and energy storage that is based on a traditional AC-Quadratic Program (AC-QP) OPF solution method. Test cases are provided to demonstrate the economic benefits of the multi-period OPF solution. The sensitivity of the cost of operation and scheduled storage charging pattern to the length of the multi-period OPF horizon chosen is assessed. Additionally, the computation time for various OPF horizons is also examined. Finally, the effect of forecast errors on the choice of OPF horizon is investigated.**

I. Introduction

The optimal power flow (OPF) problem has been well researched in the past few decades. As a result, many solution methods have been established for traditional electricity networks. One common practice is to use the DC power flow approximation to formulate the problem as a quadratic program (QP), for which reliable solvers are readily available [1]-[2]. However, while this method scales well for realistically large networks, it does not result in an AC-feasible solution and can have significant discrepancies compared to the AC solution [3]. More recently, semidefinite and second-order cone programming (SOCP) techniques have been applied to convex relaxations of the OPF problem, as in [4] and [5]. These relaxations, when tight, have the advantage that they guarantee a globally optimal solution. However, for arbitrary networks there are no guarantees that the relaxations will be tight or produce feasible solutions [6]-[7]. Furthermore, the solvers currently available do not necessarily scale well for large networks. Another solution method is the traditional AC-QP OPF algorithm, the details of which can be found in [8]. This method alternates between solving a simple quadratic program to minimize cost of generation and running an AC power flow to ensure AC-feasibility. It has the benefits of guaranteeing an AC-feasible solution, and QP solvers are available for arbitrarily large networks. These benefits come, however, with the tradeoff that the algorithm may produce locally, rather than globally, optimal solutions. Because AC feasibility is guaranteed, this solution method is the focus of this paper.

There is increasing need for integration of renewable generation sources into traditional electricity networks. Renewable sources are important for the economic and environmental operation of power systems. However, challenges arise due to their inherently variable nature. Thus, storage devices become important in the operation of these generation sources: they can charge using excess renewable energy at high production periods, and return power to the network when renewable generation is lacking [9]. By carefully scheduling these devices, they can thus reduce the impact of large fluctuations from renewable generation on network reliability. Therefore, the scheduling of storage devices must be carefully considered, which requires modifying traditional OPF methods. Including the model for storage devices, such as the one given in [10], in the OPF problem introduces temporal coupling over the OPF horizon, which results in a multi-period OPF formulation.

This multi-period OPF offers the ability to make current storage (dis)charging decisions taking into account not only current conditions, but also future forecasted conditions. Many multi-period OPF formulations that include renewable generation and storage, as in [11] and [12], use a horizon of 24 hours. The size and complexity of the multi-period OPF problem when using such a long horizon may substantially increase the computation time, thus limiting the real-time applications of the OPF tool developed. However, the length of the horizon affects the benefits that are derived from solving the multi-period OPF, as decisions seek to minimize cost over the entire horizon, not simply the cost at the current time period. Implementing a longer horizon may thus increase the quality of solution in terms of minimum cost of generation, but also makes the solution more susceptible to forecast error. This tradeoff becomes particularly important in real-time applications for realistically large networks. The paper explores various horizons, ranging from 1 hour to 8 hours, with a sampling time of half an hour. An 8-hour horizon therefore requires optimizing over 16 time steps. The results of the various horizons tested offer insights into the sensitivity of the solution to the choice of this horizon.

Research supported by the Department of Energy, ARPA-E Award No. DE-AR0000232, Green Electricity Network Integration (GENI) Program.

The organization of this paper is as follows. Section II establishes the notation used in the subsequent formulation, while Section III describes the multi-period OPF problem with storage and wind, and the AC-QP OPF solution method. Section IV describes the two test cases used to assess the performance of the proposed method. Section V gives the results of those test cases and demonstrates the sensitivity of the OPF solution to the OPF horizon, the impact that forecast errors can have on the final solution, and the inherent tradeoff between the increased complexity/computation time and economic benefits derived from using a longer OPF horizon. Conclusions are then offered in Section VI.

II. Notation

Parameters :

$\mathcal{G}$	set of conventional generation nodes
$C_i(P_{g,i})$	quadratic cost curve for each generator $i \in \mathcal{G}$
$\mathcal{S}$	set of storage nodes
$\mathcal{W}$	set of wind nodes
$\mathcal{T}$	set of time periods
T^{term}	time of day at the end of the OPF horizon
T	length in hours of OPF horizon
$\mathcal{N}$	set of nodes in the network
$slack$	slack node in the network
$W_i^{max}(t)$	available wind at node $i \in \mathcal{W}$ at time $t \in \mathcal{T}$
S_{ij}^{max}	maximum apparent power flow in line from node i to node j
$P_{g,i}^{min}, P_{g,i}^{max}$	minimum, maximum active power limits when generator at node $i \in \mathcal{G}$ in service
$Q_{g,i}^{min}, Q_{g,i}^{max}$	minimum, maximum reactive power limits when generator at node $i \in \mathcal{G}$ in service
T_s	sampling time in storage dynamics model
η_c, η_d	storage device charging, discharging efficiencies
b_i^{term}	terminal state of charge of storage at node $i \in \mathcal{S}$
$b_{i,0}$	initial state of charge of storage at node $i \in \mathcal{S}$
B_i	storage energy limit at node $i \in \mathcal{S}$
$R_{c,i}^{max}, R_{d,i}^{max}$	maximum charging, discharging of storage at node $i \in \mathcal{S}$
$\frac{\partial S_{ij}}{\partial \theta_k}(t)$, $\frac{\partial S_{ij}}{\partial V_k}(t)$	AC line flow sensitivity factors
$J(t)$	AC power flow Jacobian matrix at time $t \in \mathcal{T}$
V_i^{min}, V_i^{max}	minimum, maximum voltage magnitude at node $i \in \mathcal{N}$
γ	(nonnegative) cost coefficient penalizing the deviation of terminal state of charge of storage device $i \in \mathcal{S}$ from specified value b_i^{term}

Control Variables:

$\Delta P_{g,i}(t)$	change in active power generation at node $i \in \mathcal{G}$ at time $t \in \mathcal{T}$
$\Delta Q_{g,i}(t)$	change in reactive power generation at node $i \in \mathcal{G}$ at time $t \in \mathcal{T}$
$\Delta r_{c,i}(t), \Delta r_{d,i}(t)$	change in battery active power charging, discharging at node $i \in \mathcal{S}$ at time $t \in \mathcal{T}$
$b_i(t)$	battery energy at node $i \in \mathcal{S}$ at time $t \in \mathcal{T}$
$\Delta P_{w,i}(t)$	change in wind curtailment at node $i \in \mathcal{W}$ at time $t \in \mathcal{T}$
$\Delta V_i(t)$, $\Delta \theta_i(t)$	change in voltage magnitude, angle at node $i \in \mathcal{N}$ at time $t \in \mathcal{T}$

III. AC-QP OPF Solution Method

The following algorithm is based on the traditional AC-QP OPF method described in [8]. This method begins by solving an AC power flow from an initial operating point. In this application, the initial generation and voltage schedules come from the solution of a modified, multi-period version of the SOCP OPF relaxation given in [5] that includes both wind and storage. The full problem description of this modified SOCP relaxation can be found in [13]. The SOCP solution also provides a lower bound on the globally optimal cost of generation, which is used to assess the quality of solution coming from the AC-QP OPF method. After the initial power flow is run, the QP that follows is solved to find an operating point which minimizes the total quadratic cost of traditional generation while enforcing power balance in the network. The linearization/sensitivity terms required by this QP are obtained from the AC power flow solution. The results of the QP give the generation and voltage schedules used to run an AC power flow at the next QP-power flow iteration.

Additionally, the net of charging and discharging of each storage device in the QP solution is used to determine the (dis)charging status of that device. That status is then enforced in the QP solved at the next iteration by setting the appropriate charging or discharging limit of that device to be 0; this eliminates the possibility of simultaneous charging and discharging of storage devices in the QP solution. The status is then updated after each subsequent QP solution. A more detailed discussion of this processing step can be found in [14]. This approach explicitly enforces storage complementarity, while avoiding the use of binary variables. The successive linearization procedure then continues, alternating between solving a full AC power flow and the QP until the two solutions agree within a specified tolerance. The overall AC-QP solution method is summarized in Figure 1.

The QP solved at each iteration makes use of the power flow linearization:

$$J(t) = \begin{bmatrix} \frac{\partial P}{\partial \theta}(t) & \frac{\partial P}{\partial V}(t) \\ \frac{\partial Q}{\partial \theta}(t) & \frac{\partial Q}{\partial V}(t) \end{bmatrix}, \qquad \Delta x(t) = \begin{bmatrix} \Delta\theta(t) \\ \Delta V(t) \end{bmatrix}$$

$$\Delta S(t) = \begin{bmatrix} \Delta P_g(t) - \Delta r_c(t) - \Delta r_d(t) - \Delta P_w(t) \\ \Delta Q_g(t) \end{bmatrix}$$

and is formulated as:

$$\min \sum_{t\in\mathcal{T}} \sum_{i\in\mathcal{G}} C_i(P_{g,i}^0 + \Delta P_{g,i}, t) + \gamma \sum_{i\in\mathcal{S}} \|b_i(T) - b_i^{term}(T^{term})\|_2^2 \quad (1a)$$

subject to ($\forall t \in \mathcal{T}$):

$$J(t)\Delta x(t) = \Delta S(t) \quad (1b)$$

$$P_{g,i}^{min} \le P_{g,i}^0(t) + \Delta P_{g,i}(t) \le P_{g,i}^{max}, \quad \forall i \in \mathcal{G} \quad (1c)$$

$$Q_{g,i}^{min} \le Q_{g,i}^0(t) + \Delta Q_{g,i}(t) \le Q_{g,i}^{max}, \quad \forall i \in \mathcal{G} \quad (1d)$$

$$\Delta\theta_{slack}(t) = 0 \quad (1e)$$

$$-\pi \le \theta_i^0(t) + \Delta\theta_i(t) \le \pi, \quad \forall i \in \{\mathcal{N}\backslash slack\} \quad (1f)$$

$$V_i^{min} \le V_i^0(t) + \Delta V_i(t) \le V_i^{max}, \quad \forall i \in \mathcal{N} \quad (1g)$$

$$0 \le P_{w,i}^0(t) + \Delta P_{w,i}(t) \le W_i^{max}(t), \quad \forall i \in \mathcal{W} \quad (1h)$$

$$b_i(0) = b_{i,0}, \quad \forall i \in \mathcal{S} \quad (1i)$$

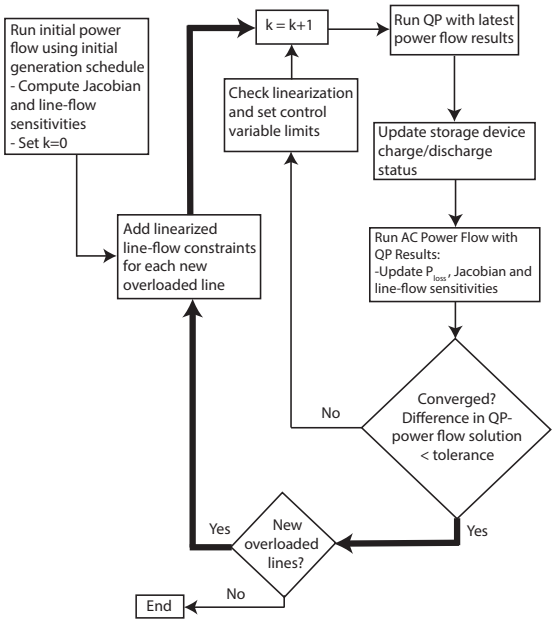

Fig. 1. AC-QP OPF Iterative Method

$$b_i(t+1) = b_i(t) + T_s\eta_c(r^0_{c,i}(t) + \Delta r_{c,i}(t)) - \frac{T_s}{\eta_d}(r^0_{d,i}(t) + \Delta r_{d,i}(t)), \quad \forall i \in \mathcal{S} \tag{1j}$$

$$0 \le r^0_{c,i}(t) + \Delta r_{c,i}(t) \le R^{max}_{c,i}, \quad \forall i \in \mathcal{S} \tag{1k}$$

$$0 \le r^0_{d,i}(t) + \Delta r_{d,i}(t) \le R^{max}_{d,i}, \quad \forall i \in \mathcal{S} \tag{1l}$$

$$0 \le b_i(t) \le B_i, \quad \forall i \in \mathcal{S}. \tag{1m}$$

Quantities with a superscript '0' in the QP denote results from the AC power flow, and are updated after each QP-power flow iteration. Additionally, (1i)–(1m) model the storage state of charge dynamics with non-ideal charging and discharging efficiencies, as described in [10].

A penalty term is added to the generation cost term of the OPF objective to avoid the greedy use of storage. This is of particular importance for shorter horizon choices. The intuitive use of storage is to charge devices during low demand and high renewable periods of the day, and then discharge them during high demand and low renewable periods to achieve peak shaving and reduce the total operating cost. However, shorter horizons may not achieve this desirable behavior, as the valley and peak periods are not visible within the reduced optimization horizon.

To address this problem, a reference storage usage pattern can be determined by solving a higher level problem, such as unit commitment, that performs an optimization over a sufficiently long horizon. The approach adopted has been to establish this reference trajectory by solving a higher-level, approximate, storage allocation problem using six 4-hour time steps.

The multi-period OPF seeks to minimize the total generation cost over the horizon of interest. To do so, it can use storage freely, and only incurs a penalty cost if the state of charge of each storage device at the end of the horizon deviates from the reference usage pattern. This terminal penalty also ensures fair usage of storage devices over the entire day. As storage devices begin the 24 hours charged to half of their energy rating, they should be returned to that initial value at the end of the 24-hour period. This is achieved by varying the penalty coefficient γ throughout the 24 hours, depending on the time at the end of the OPF horizon, according to the following scheme:

$$\gamma = \begin{cases} 10^2, & T^{term} \in [1, 15] \\ 10^3, & T^{term} \in (15, 17] \\ 10^4, & T^{term} \in (17, 19] \\ 10^5, & T^{term} \in (19, 21] \\ 10^6, & T^{term} \in (21, 24] \\ 10^2, & T^{term} > 24. \end{cases} \tag{2}$$

This coefficient is relatively low for the first part of the day and then gradually increases as the day progresses. The specific values given above are designed such that the largest coefficient is of the same order of magnitude as the cost of conventional generation. Additionally, including several steps to increase this penalty coefficient ensures a relatively smooth transition to return storage energy levels at the end of the 24 hours to their initial values. Moreover, the very large coefficient over the last few hours ensures that if it is feasible to do so, the state of charge of each storage device will be returned to its initial value.

Finally, apparent power line flow limits are enforced by including a linearized line flow constraint,

$$S^0_{ij}(t) + \sum_{k\in\mathcal{N}} \frac{\partial S_{ij}}{\partial \theta_k}(t)\Delta\theta_k(t) + \sum_{k\in\mathcal{N}} \frac{\partial S_{ij}}{\partial V_k}(t)\Delta V_k(t) \le S^{max}_{ij} \tag{3}$$

in the QP for every line that is at or above 95% of its line flow limit after the initial power flow. Additional line flow constraints are then included as necessary for any further overloaded lines in subsequent QP-power flow iterations.

The convergence of this method depends on the accuracy of the linearization used in the QP at each iteration. To improve the convergence of this method, a step is added to check the accuracy of the linearization before the QP is solved at each iteration. This additional step is based on the trust-region formulation provided in [15]. After each power flow is solved, the actual change in system losses,

$$\Delta P_{loss\_act}(t) = P^k_{loss}(t) - P^{k-1}_{loss}(t), \tag{4}$$

is compared to the predicted change in losses from the QP solution,

$$\Delta P_{loss\_pred}(t) = \sum_{i\in\mathcal{N}}\sum_{k\in\mathcal{N}} \left[\frac{\partial P_i}{\partial \theta_k}(t)\Delta\theta_k(t) + \frac{\partial P_i}{\partial V_k}(t)\Delta V_k(t)\right] \tag{5}$$

for every time period in the multiperiod OPF horizon. If they are within a specified tolerance, the linearization is considered sufficiently accurate. If, however, the predicted and actual changes in system losses do not closely agree, the linearization is not considered sufficiently accurate, and the constraints on control variable updates are reduced by a scaling factor. This reduces the magnitude of allowable control variable changes,

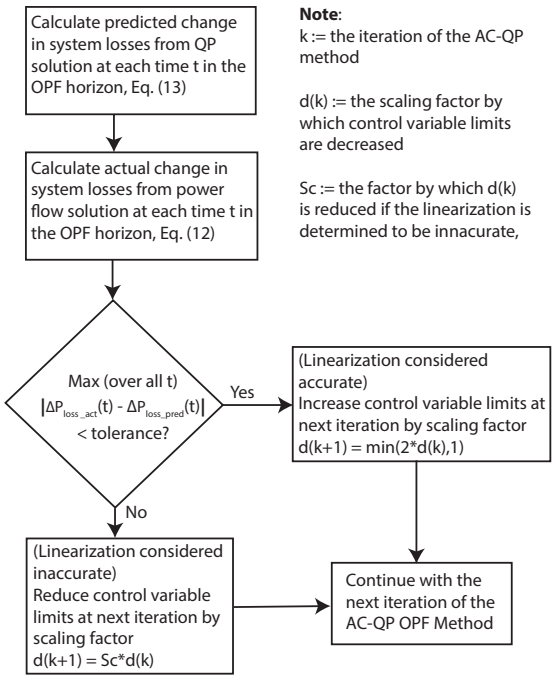

Fig. 2. Trust Region Step of AC-QP OPF Method

which improves convergence reliability. The details of this step are summarized in Figure 2. In the following investigations, a reduction factor of $Sc = 0.5$ was sufficient to provide acceptable convergence rates.

IV. Test Cases

Two test cases are presented to assess the performance of the proposed method. They are both based on a modified version of the Polish 3012wp network, which can be found in [16]. This system has been augmented with both wind nodes and storage devices. Three hundred storage devices were placed at randomly chosen locations within the network. The maximum (dis)charging rating and maximum energy rating of each device were then chosen to be randomly distributed over the ranges 1–5 MW and 1–20 MWh, respectively. One hundred wind locations were randomly chosen within the network. The available wind at those locations was likewise chosen such that they were randomly distributed over 1–100 MW. To create a demand profile over 24 hours, the hourly load data provided in the RTS-96 test case description for a summer weekend was used [17]. Both cases are assumed to begin at 7 p.m., just after the peak demand period has occurred. Additionally, it is assumed that storage devices begin each 24-hour period charged to half of their maximum energy ratings, and must be returned to that value by the end of the 24-hour period to maintain a fair usage policy. The demand and wind profiles assumed in this case over the course of 24 hours are given by the solid lines in Figure 3.

Both test cases presented use the same network description, as well as randomly chosen wind and storage device locations and ratings. The difference between the two cases is in

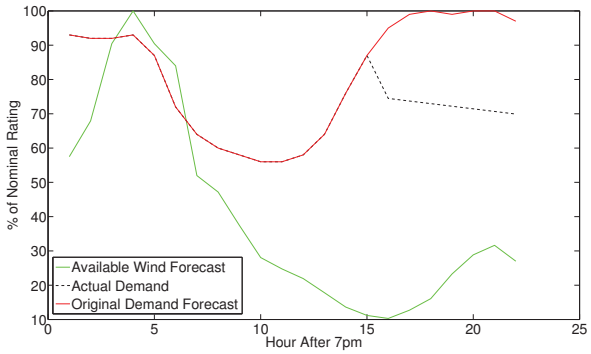

Fig. 3. Demand and Wind Profiles Used in Both Test Cases

the assumption of load and wind forecast accuracy. Initially, results are presented assuming perfect wind and load forecasts. This test case is used to assess the computational scalability of the method and to demonstrate the sensitivity of the total cost of generation to the OPF horizon chosen. The second test case introduces an event such that the load forecast has significant error, as shown by the dotted line in Figure 3. This case highlights the sensitivity of the OPF solution to forecast errors, and considers the effect of horizon length.

V. Results and Discussion

A. Test Case 1: Perfect Wind and Load Forecasts

The results of the first test case are given in Figures 4–9. Both the total cost of generation and total stored energy of all 300 storage devices over the 24-hour period considered are given in Figure 4. The storage state of charge reference pattern over the entire day, denoted by T=24 in the lower figure, establishes the terminal value that is used in the penalty term in the OPF objective function (1a).

Figure 4 demonstrates the improved performance of the longer OPF horizons in scheduling storage (dis)charging. Shorter horizons, such as 1 or 2 hours, result in storage charging over the valley period (hours 7–13) being insufficiently scheduled, such that during the peak demand period (hours 15–24) less storage is available to achieve lower peak operating costs. This highlights the short-sighted nature of these horizons that are unable to anticipate the upcoming peak demand. It should also be observed that these shorter horizons not only charge storage devices to a lower state of charge, but also begin discharging several hours before the peak demand period, contributing to a higher cost of operation. Conversely, longer horizons, such as 4, 6 or 8 hours, successfully charge storage devices to a higher state of charge level before the peak demand period. Storage can then be discharged during the peak periods, resulting in significant cost savings.

Figure 5 highlights the economic improvement for each horizon tested, relative to the cost of operation with no storage in the network. Both the 1- and 2-hour horizons achieve some cost savings during hours 14–16, but they also incur higher cost during the high-demand hours of 19–21, as storage must be charged to return to its initial state of charge. However,

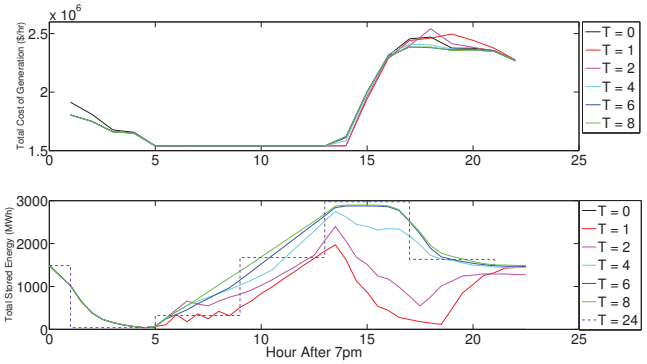

Fig. 4. Case 1: Cost of Generation and Total Stored Energy Results

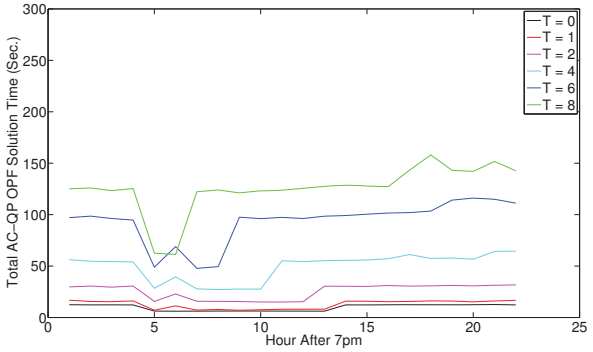

Fig. 7. Case 1: AC-QP OPF Timing Results

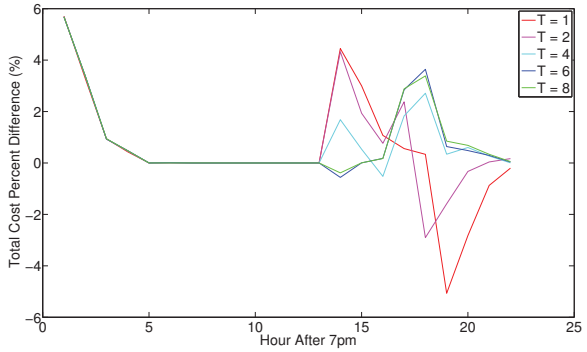

Fig. 5. Case 1: Hourly Percent Savings Compared to No Storage Case

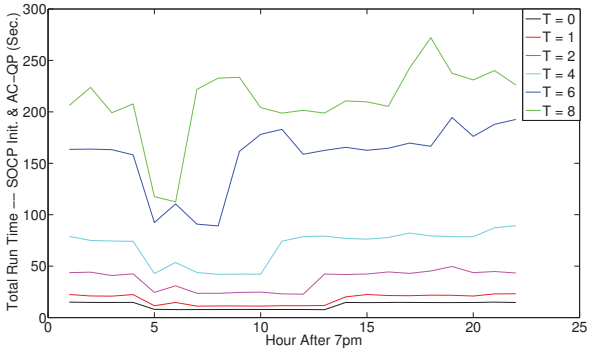

Fig. 8. Case 1: SOCP Initialization and AC-QP Total Timing Results

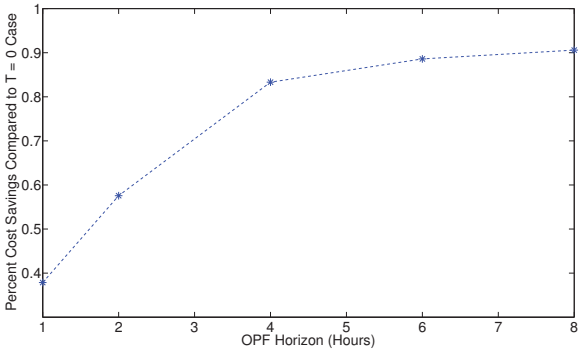

Fig. 6. Case 1: Total Cost Percent Savings Over 24 Hours for Various Horizons

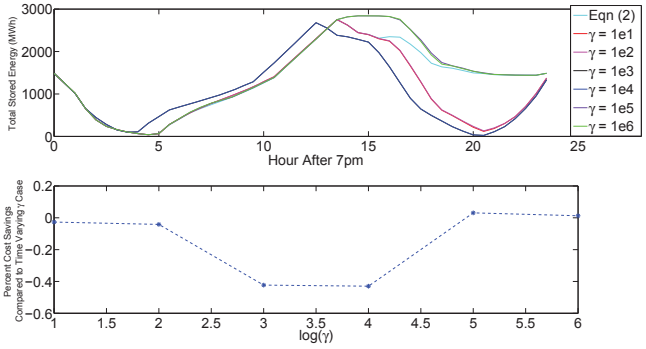

Fig. 9. Case 1: Total Energy and Cost Comparison - Constant γ, $T = 4$

using a longer horizon, such as 4, 6, or 8 hours, avoids this issue and can achieve cost savings up to 4% during peak demand periods in this case. Figure 6 shows the improved cost savings over an entire day that result from optimally scheduling storage (dis)charging. The savings can be up to 0.9% per day in this case. While longer horizons produce higher cost savings, there is a diminishing benefit as the length of the OPF horizon is increased.

Figures 7–8 show the computation time for various OPF horizons. For real-time OPF applications, an execution time target of 5 minutes is assumed. While longer horizons can schedule storage devices more economically, the computation time of the AC-QP OPF method increases significantly as the horizon increases, as shown in Figure 7. Moreover, when the initialization time to solve the SOCP OPF relaxation is considered in the total computation time, as shown in Figure 8, the increase in total time for longer OPF horizons is even more pronounced. Horizons longer than 8 hours have not been considered as they are likely to exceed the 5 minute target assumed for real-time applications. Computation time must be carefully addressed when choosing an appropriate horizon, especially considering the diminishing cost benefits achieved with longer horizons.

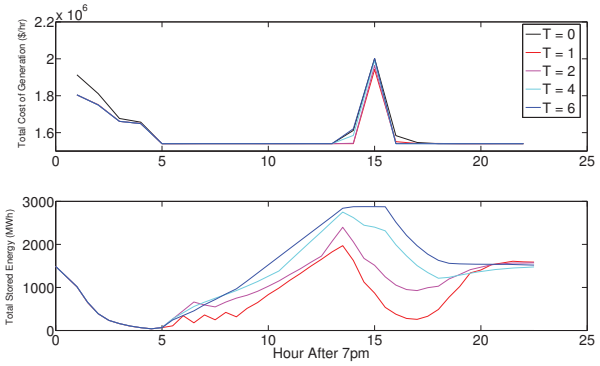

Fig. 10. Case 2 Cost of Generation and Total Stored Energy Results

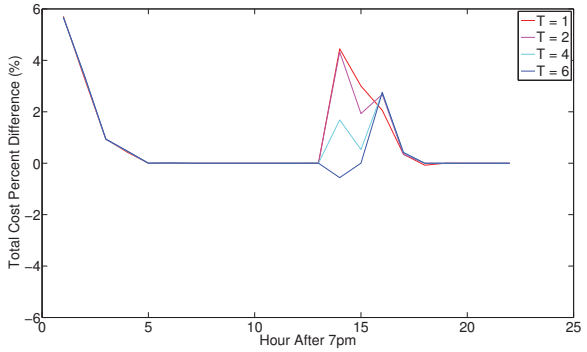

Fig. 11. Case 2 Hourly Percent Savings Compared to No Storage Case

Figure 9 shows the sensitivity of these results to the choice of the storage terminal penalty coefficient γ. The first test case is repeated for a constant choice of γ throughout the day and a horizon of 4 hours. When γ is less than 10^4, storage is discharged before the peak demand period. This short-sighted operation of storage leads to a higher operating cost over the entire day, compared to the time-varying scheme proposed. Conversely, when γ is increased to 10^5 or 10^6, the storage usage pattern matches the reference pattern more closely. This leads to a slightly lower cost of operation compared to the time-varying scheme. However, this result relies upon the assumption of having a perfect demand forecast.

B. Test Case 2: Introducing Load Forecast Error

The second test case, the results of which are summarized in Figures 10–13, explores the impact of significant forecast errors on the quality of solutions for various OPF horizons. As the day begins, the wind and demand forecasts are those given by the solid lines in Figure 3. Then, at hour 16, a new demand forecast is received, which is shown by the dotted curve in Figure 3. Comparing the original forecast and actual demand curves, it it observed that there is significant error in the original forecast. In particular, the actual demand lacks the peak demand period that was originally anticipated. The degree to which this forecast error impacts the quality of the solutions achieved by the AC-QP OPF depends on the horizon chosen, as shown in Figure 10.

As in the first case, storage devices begin charging at hour 5. The longer horizons (4 and 6 hours) charge those devices more rapidly, and have them more fully charged by hour 14. This is due to the fact that those horizons are sufficiently long for the peak demand at hour 16 to be anticipated. However, the shorter horizons (1 and 2 hours) begin charging, but at a lower rate, as the peak demand has not yet been taken into account. As in the first case, the shorter horizon results are short-sighted, and so begin discharging storage devices at hour 14. In this case, however, the demand forecast for which the storage (dis)charging pattern was planned was in error. An event occurs at hour 16 such that a large portion of the anticipated demand does not eventuate, and load continues to decrease over the rest of the day. Consequently, the original

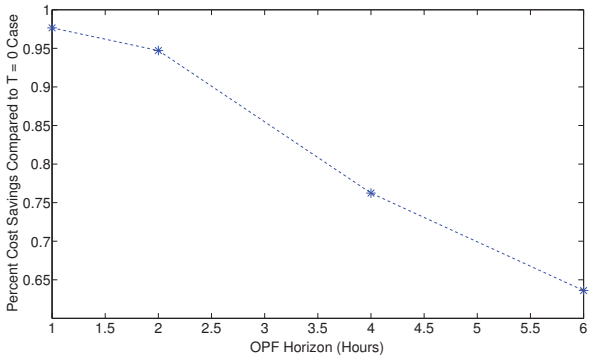

Fig. 12. Case 2 Total Cost Percent Savings Over 24 Hours for Various Horizons

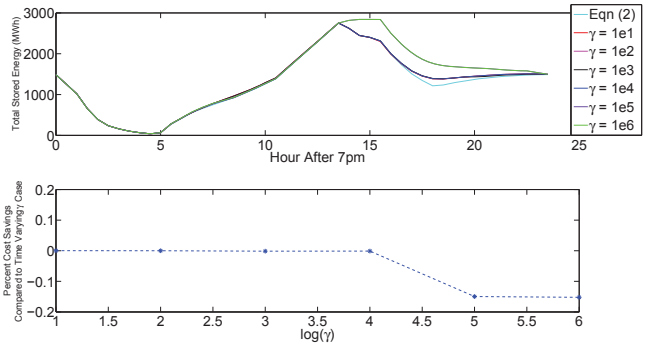

Fig. 13. Case 2 Total Energy and Cost Comparison - Constant γ, $T = 4$

peak demand period never occurs. The longer horizons have already incurred the extra cost of charging storage to a higher level in planning for that peak, which results in a higher cost compared to the shorter horizon results. This is just one example where relying upon a longer horizon, which is more economic given a reliable forecast, leaves operations vulnerable to forecast error and actually results in a higher cost solution.

Figure 11 emphasizes the impact that forecast error may have on the cost savings achieved by adding storage to a network. Compared to the case without any storage in the

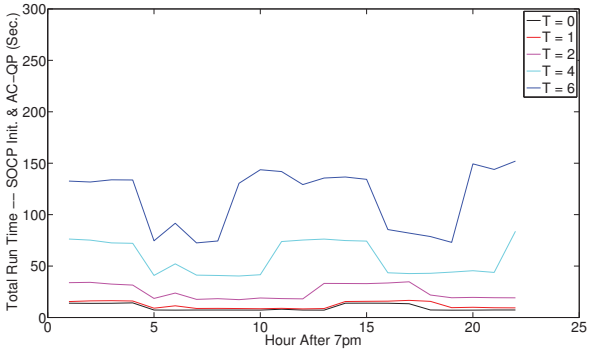

Fig. 14. Case 2 SOCP Initialization and AC-QP Total Timing Results

network, all horizons achieve similar cost savings until hour 14. At that time, the longer horizons incur a cost to charge storage to a higher energy level, while the shorter horizons achieve cost savings up to 4.5% in this case, as they have already begun returning power from storage devices to the network. Then, after the unanticipated load-reduction event at hour 16, all horizons use the available storage to return power to the network. It is again clear that shorter horizons may be beneficial in scenarios with less reliable forecasts.

Considering the cost of operation over the entire 24-hour period, Figure 12 emphasizes the significance of forecast error on the quality of the solution. This plot shows that the difference in cost of operation between a 1-hour and 6-hour horizon is approximately 0.3%. In the presence of significant error, using a 1-hour horizon could save almost 1% per day. Forecast errors should also be taken into account when choosing appropriate values for γ. Figure 13 shows the results of this second case study for a constant γ throughout the day. In the presence of significant forecast errors, choices of γ that are less than 10^4 achieve the same use of storage and cost of operation as the time-varying scheme (2). However, when γ is increased to 10^5 or 10^6, while the use of storage more closely matches the reference pattern, the cost of operation is higher compared to the time-varying scheme. Placing such large penalties on deviation from terminal state of charge reduces the flexibility of the storage to adapt to forecast errors.

Taken together, these figures reveal that the degree of confidence placed in a demand or wind forecast must be assessed carefully, as that accuracy can have a significant impact on the choice of horizon length. Finally, as in the first test case, Figure 14 demonstrates the scalability of this method for a realistically large network, as all cases are within the 5-minute limit set for real-time applications. It should also be noted that if large forecast errors are a concern and shorter horizons are implemented, significant execution time savings can be achieved.

VI. Conclusions

The traditional AC-QP OPF solution method has been extended to a multi-period formulation to include both renewable generation and energy storage devices. Several factors influencing the choice of OPF horizon have been explored. First, when forecasts are accurate, longer horizons offer significant benefits in reducing operational costs. Conversely, when large forecast errors are anticipated, choosing a longer horizon may increase the operational cost, while shorter horizons can achieve greater cost savings. Together, these investigations demonstrate that optimal scheduling is reliant upon matching the horizon length to the forecast quality.

The scalability of the proposed approach has been demonstrated on a realistically large network and timing results fall within a reasonable (5-minute) operation time limit.

References

[1] A. Motto, F. Galiana, A. Conejo, and J. Arroyo, "Network-constrained multiperiod auction for a pool-based electricity market," *IEEE Transactions on Power Systems*, vol. 17, no. 3, pp. 646–653, August 2002.

[2] T. Overbye, X. Cheng, and Y. Sun, "A comparison of the AC and DC power flow model for LMP calculations," in *Proceedings of the 37th Hawaii International Conference on System Sciences*, 2006.

[3] B. Stott, J. Jardim, and O. Alsac, "DC power flow revisited," *IEEE Transactions on Power Systems*, vol. 24, no. 3, pp. 1290–1300, August 2009.

[4] J. Lavaei and S. Low, "Zero duality gap in optimal power flow problem," *IEEE Transactions on Power Systems*, vol. 27, no. 1, pp. 92–107, February 2012.

[5] S. Low, "Convex relaxation of optimal power flows part I: Formulations and equivalence," *IEEE Transactions on Control of Network Systems*, vol. 1, no. 1, pp. 15–27, March 2014.

[6] B. Lesieutre, D. Molzahn, A. Borden, and C. DeMarco, "Examining the limits of the application of semidefinite programming to power flow problems," in *Proceedings of the Allerton Conference*, Allerton House, UIUC, Illinois, 2011, pp. 1492–1499.

[7] D. Molzahn, B. Lesieutre, and C. DeMarco, "Investigation of non-zero duality gap solutions to a semidefinite relaxation of the optimal power flow problem," in *Proceedings of the 47th Hawaii International Conference on System Science*, 2014.

[8] A. Wood, B. Wollenberg, and G. B. Sheble, *Power Generation, Operation and Control*, 3rd ed. New York: John Wiley and Sons, Inc., 2013.

[9] K. Chandy, S. Low, U. Topcu, and H. Xu, "A simple optimal power flow model with energy storage," in *Proceedings of the IEEE Conference on Decision and Control*, Atlanta, GA, 2010, pp. 1051–1057.

[10] M. Almassalkhi and I. Hiskens, "Cascade mitigation in energy hub networks," in *Proceedings of the IEEE Conference on Decision and Control*, Orlando, FL, 2011, pp. 2181–2188.

[11] N. Nguyen, D. Bovo, and A. Berizzi, "Optimal power flow with energy storage systems: Single-period model vs. multi-period model," in *Proceedings of the 2015 IEEE Eindhoven PowerTech Conference*, 2015.

[12] R. Jabr, S. Karaki, and J. Korbane, "Robust multi-period OPF with storage and renewables," *IEEE Transactions on Power Systems*, vol. 30, no. 5, pp. 2790–2799, September 2015.

[13] J. F. Marley, D. K. Molzahn, and I. A. Hiskens, "An improved initialization for the AC-QP OPF method using an SOCP relaxation," *IEEE Transactions on Power Systems*, submitted.

[14] J. K. Felder and I. A. Hiskens, "Optimal power flow with storage," in *Proceedings of the Power Systems Computation Conference*, 2014.

[15] A. M. Giacomoni and B. F. Wollenberg, "Linear programming optimal power flow utilizing a trust region method," in *Proceedings of the North American Power Symposium*, 2010.

[16] R. D. Zimmerman, C. E. Murillo-Snchez, and R. J. Thomas, "Matpower: Steady-state operations, planning and analysis tools for power systems research and education," *IEEE Transactions on Power Systems*, vol. 26, no. 1, pp. 12–19, February 2011.

[17] C. Grigg, P. Wong, P. Albrecht, R. Allan, M. Bhavaraju, R. Billinton, Q. Chen, C. Fong, S. Haddad, S. Kuruganty, W. Li, R. Mukerji, D. Patton, N. Rau, D. Reppen, A. Schneider, M. Shahidehpour, and C. Singh, "The IEEE reliability test system - 1996," *IEEE Transactions on Power Systems*, vol. 14, no. 3, pp. 1010–1020, August 1999.